

Article

# Divalent Yb Doped Silica Glass and Fiber with High Quantum Efficiency for White Light Source

Changming Xia<sup>1, 2\*</sup>, Jiantao Liu<sup>2</sup>, Zhiyun Hou<sup>1, 2</sup> AND Guiyao Zhou<sup>1, 2</sup>

<sup>1</sup> Guangdong Province Key Laboratory of Nano-photonic Functional Materials and Devices, South China Normal University, Guangzhou, 510006, China

<sup>2</sup> Guangzhou Key Laboratory for Special Fiber Photonic Devices and Applications, South China Normal University, Guangzhou, 510006, China

\*Corresponding Author: xiacmm@126.com

**Abstract:** In this study, divalent Yb<sup>2+</sup>-doped silica fiber was fabricated using rod-in-tube technology. The fiber core of Yb<sup>2+</sup>-doped silica glass was prepared by high-temperature melting technology under vacuum conditions. The spectroscopic properties of the Yb<sup>2+</sup>-doped glass and fiber were studied. The experiments indicate that divalent Yb<sup>2+</sup>-doped glass has a high quantum efficiency and superbroadband fluorescence in the visible region with an excitation wavelength of 405 nm. In addition, the results suggest that Yb<sup>2+</sup>-doped fiber has a potential for application in visible fiber laser and fiber amplification.

**Keywords:** Yb<sup>2+</sup> doped glass; fiber laser; visible-infrared lasers; white light source; rod in tube

## 1. Introduction

In recent years, divalent Yb<sup>2+</sup> ions have attracted considerable interest <sup>[1]</sup> because they provide the photodarkening effect, which is a key limitation of high-power fiber lasers <sup>[2, 3]</sup>. Moreover, divalent Yb<sup>2+</sup> ions have potential applications as white light sources <sup>[4]</sup>. The optical properties of Yb<sup>2+</sup> ions in crystalline materials, such as CaF<sub>2</sub> <sup>[5, 6]</sup>, SrI<sub>2</sub> <sup>[7]</sup>, MgF<sub>2</sub> <sup>[8]</sup>, YAG (Y<sub>3</sub>Al<sub>5</sub>O<sub>12</sub>, YAlO<sub>3</sub>) <sup>[9]</sup>, NaI <sup>[10]</sup>, phosphate crystals <sup>[11]</sup>, and LiBaF<sub>3</sub> <sup>[9]</sup> have been widely reported. In addition, the optical properties of Yb<sup>2+</sup> ions in materials such as aluminosilicate glass <sup>[12]</sup> and silica glass <sup>[13, 14]</sup> have also been widely investigated. However, the laser performance of Yb<sup>2+</sup> ions has not been investigated because of the high excited-state absorption of these ions.

The ground state configuration of Yb<sup>2+</sup> ions is 4f<sup>14</sup>, whose excited state configuration is 4f<sup>13</sup>5d<sup>1</sup> and consists of 140 energy levels. In addition, the state level of 4f<sup>13</sup>6s<sup>1</sup> is the lowest excited energy level of the Yb<sup>2+</sup> ions. However, in most materials, the 4f<sup>13</sup>6s<sup>1</sup> energy level is lower than the 4f<sup>13</sup>5d<sup>1</sup> level; therefore, there is excited-state absorption, which hinders laser oscillation. This is a limitation for laser development of the Yb<sup>2+</sup> doped material. Therefore, a material with the lowest excited level that belongs to the 4f<sup>13</sup>5d<sup>1</sup> configuration is necessary. S. Kück believes that materials with a large crystal field can be used <sup>[1]</sup>. Here, the 4f<sup>13</sup>5d<sup>1</sup> level largely splits, resulting in a 4f<sup>13</sup>5d<sup>1</sup> level lower than the 4f<sup>13</sup>6s<sup>1</sup> level.

In this study, the divalent Yb<sup>2+</sup>-doped silica fiber was fabricated by rod-in-tube technology. The fiber core of Yb<sup>2+</sup>-doped silica glass was prepared by high-temperature melting technology under vacuum conditions. The spectroscopic

properties of the  $\text{Yb}^{2+}$ -doped glass and fiber were studied. The experiments indicate that the  $\text{Yb}^{2+}$ -doped glass has a high quantum efficiency, and  $\text{Yb}^{2+}$ -doped fiber has a potential application in visible fiber lasers. The laser performances of the divalent  $\text{Yb}^{2+}$ -doped fibers were measured. The results suggest that in the future  $\text{Yb}^{2+}$ -doped fiber can be widely applied in the development of fiber laser and fiber amplification operating in the visible region.

## 2.Experimental

The  $\text{Yb}^{2+}$ -doped fiber was fabricated by rod-in-tube technology. The fiber core was  $\text{Yb}^{2+}$ -doped silica glass with a composition of 97.95SiO<sub>2</sub>-1.86Al<sub>2</sub>O<sub>3</sub>-0.19Yb<sub>2</sub>O<sub>3</sub> (mol%), and was prepared by the traditional melting technology under the high temperature of 1800 °C using a graphite crucible. Graphite has intensity reduction properties under high temperature, which can promote the reduction of trivalent  $\text{Yb}^{3+}$  to divalent  $\text{Yb}^{2+}$  ions [4, 15]. The absorption spectrum was recorded with an ocean optical spectrophotometer Maya 2000 in the range of 200–1100 nm, and a light source (DH-2000-BAL, ocean optics) was used. The excitation spectrum with the emission centred at 541 nm and emission spectrum under the excitation of 365, 405, and 427 nm were measured with an Edinburgh FL-FS 920 TCSPC, in which a Xenon lamp in the range of 200–850 nm was used as the excitation source. The fluorescence lifetime was measured using the Edinburgh FL-FS 920 TCSPC [16, 17]. The quantum efficiency was recorded with a commercialised system (XPQY-EQE-350-1100, Guangzhou Xi Pu Optoelectronics Technology Co., Ltd.) [18]. The refractive index profile of the  $\text{Yb}^{2+}$ -doped fiber was measured with a digital holographic system [19].

## 3.Results and discussion

The  $\text{Yb}^{2+}$ -doped silica glass sample, shown in Figure 1, present brownish yellow colouring, which can be attributed to the characteristic absorption of  $\text{Yb}^{2+}$  ions in ultraviolet (UV) to visible spectral range, which is in agreement with the reference [8].



**Figure 1.**  $\text{Yb}^{2+}$  doped silica glass samples.

UV-visible-near-infrared absorption of  $\text{Yb}^{2+}$ -doped silica glass and photoluminescence spectra with excitation of 365 nm is shown in Figure 2. The  $\text{Yb}^{2+}$ -doped silica glass has intensity absorption in the UV-visible region, and this absorption band extends to the near-infrared region. In addition, there is a small absorption band at 976 nm corresponding to the characteristic f-f band transition of  $\text{Yb}^{3+}$  ions, which suggests the presence of few  $\text{Yb}^{3+}$  ions. A broad emission band centred at 542 nm is observed when it is excited with a wavelength of 365 nm in response to the 4f<sup>13</sup>5d -4f<sup>14</sup> transition [20]. The band width is up to 155 nm, which suggests that  $\text{Yb}^{2+}$ -doped silica glasses have outstanding optical properties. The  $\text{Yb}^{2+}$ -doped silica glass exhibits photoluminescence quantum yields (QY) of 68.8% and 69.2% with excitations of 365 and 405 nm, respectively, which suggests a

potential for use as a visible laser. Figure 3a shows the excitation spectrum with emission wavelength of 540 nm and Figure 3b shows the emission spectra with excitation wavelengths of 365, 405, and 427 nm of the  $\text{Yb}^{2+}$  doped silica glass.

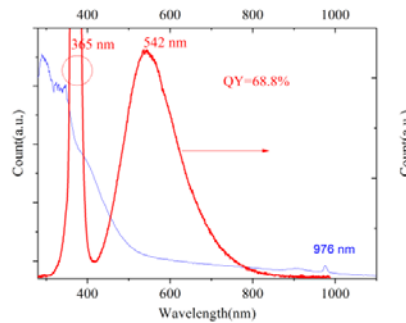


**Figure 2.** UV-near-infrared absorption and photoluminescence spectra with 365 nm excitation.

From Figure 3a, there are three excitation wavelengths centred at 282, 365, and 434 nm corresponding to the  $5\text{d}-4\text{f}^{13}5\text{d}$  transition [20], and the excitation intensity of 434 nm is the largest. In Figure 3b, the emission peak was centred at 543, 534, and 541 nm when the excitation wavelength was located at 365, 405, and 427 nm, respectively. The emission bandwidths for the excitation wavelengths of 365, 405, and 427 nm were 209, 163, and 159 nm, respectively, which corresponds to the double of the values reported in reference [8].

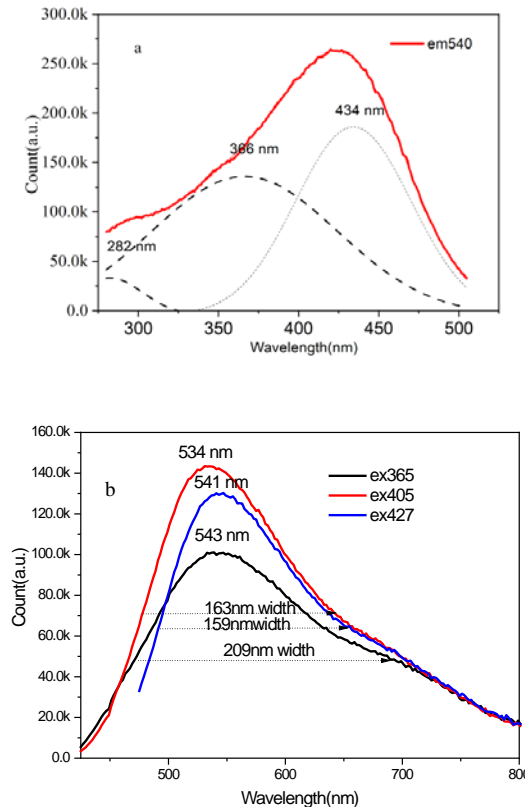
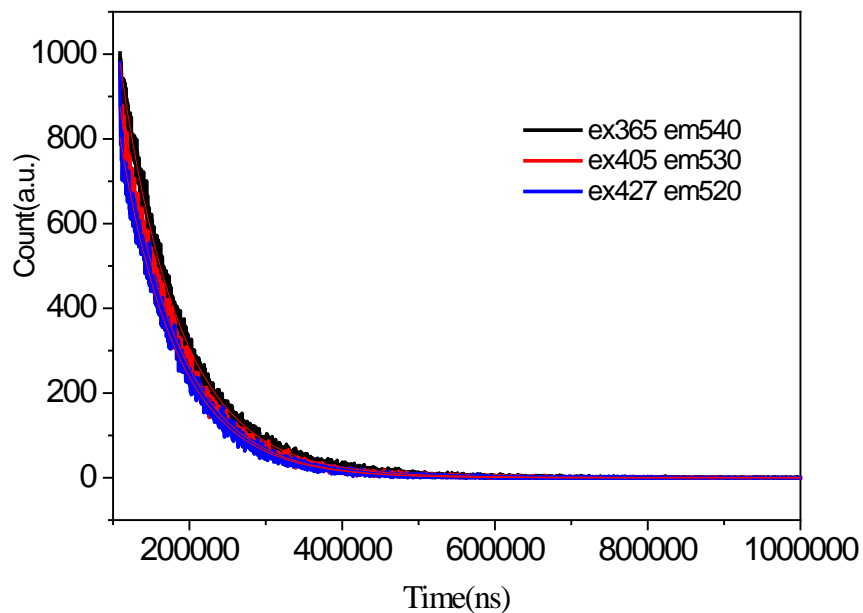


**Figure 3.** Excitation and emission spectra of  $\text{Yb}^{2+}$  doped silica glass. (a) Excitation spectrum with emission wavelength of 540 nm; (b) emission spectra with excitation wavelengths of 365, 405, and 427 nm.

The lifetime of  $\text{Yb}^{2+}$ -doped silica glass was monitored at 540, 530 and 520 nm and adjusted to single exponential functions, as shown in Figure 4. The lifetimes were 78.048, 74.582, and 74.569  $\mu\text{s}$  monitored at 540, 530, and 520 nm, when the excitation wavelengths were 365, 405, and 427 nm, respectively. Using the lifetimes and quantum efficiency, the emission cross-section  $\sigma_{\text{em}}$  can be obtained with the McCumber formula [8]:

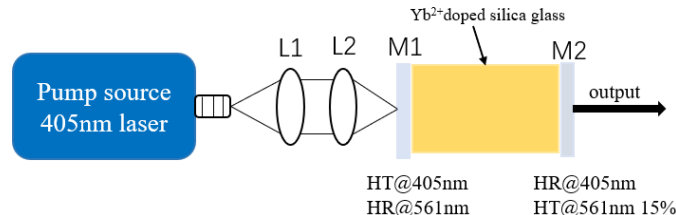
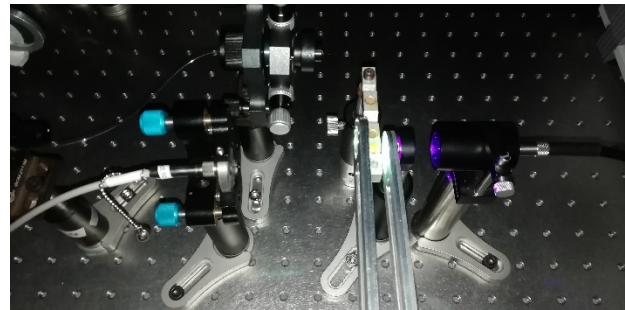
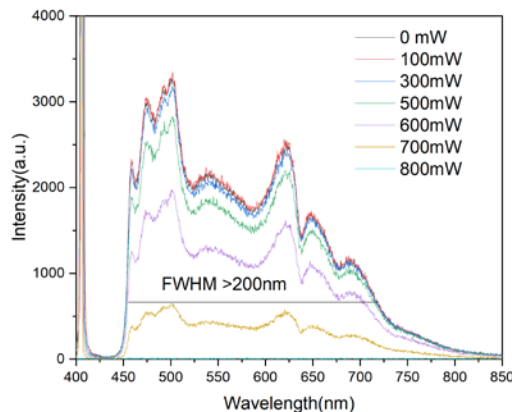
$$\sigma_{\text{em}} = \eta \sqrt{\frac{\ln 2}{\pi}} \frac{1}{4\pi c n^2 \tau} \frac{\lambda^4}{\Delta\lambda} \quad (1)$$

where  $\eta$  is the quantum efficiency,  $c$  is the speed of light,  $n$  is the refractive index,  $\tau$  is the emission lifetime,  $\lambda$  is the peak emission wavelength, and  $\Delta\lambda$  is the emission bandwidth. According to the results, the emission cross-sections of the excitation wavelength at 365 and 405 nm are  $2.13825 \times 10^{-19}$  and  $2.69916 \times 10^{-23} \text{ cm}^2$ , respectively, which are higher than those of  $\text{Yb}^{2+}:\text{MgF}_2$ , but smaller than those of  $\text{Yb}^{2+}:\text{KMgF}_3$ , reported in reference [8].



**Figure 4.** Lifetimes of  $\text{Yb}^{2+}$ -doped silica glass monitored at 540, 530 and 520 nm when the excitation wavelength was of 365, 405, and 427 nm.

$\text{Yb}^{2+}$ -doped glass with a thickness of 3 mm was used for laser with 405 nm pumping. The surface of glass was optically polished. A simple laser with F-P cavity was constructed with two dichroic mirrors with high reflectivity (>99% and 85%) at 561 nm as shown in Figure 5. However, instead of the laser, a superbroadband fluorescence in the visible region from 445 to 800 nm was obtained, with bandwidth of more than 200 nm. Figure 5c shows the emission spectra of glass with different pump powers. The intensity of the spectra increased with increasing pump laser intensity. Figure 6 shows a photograph of a harsh white light emitted from the glass with an excitation wavelength of 405 nm.

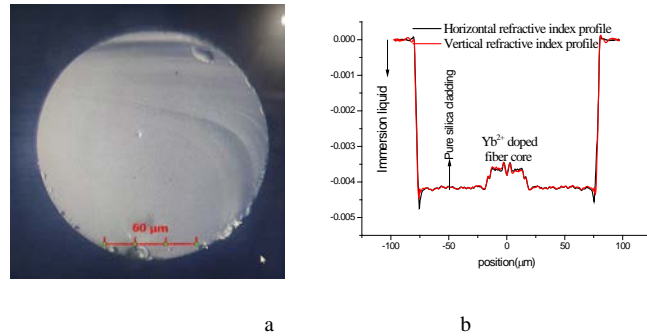
(a) Scheme of Yb<sup>2+</sup>-doped glass laser(b) A simple glass solid laser cavity set up with Yb<sup>2+</sup> glass(c) Superbroadband fluorescence of Yb<sup>2+</sup>-doped glass

**Figure 5.** (a) Scheme of Yb<sup>2+</sup>-doped glass laser, (b) A simple glass solid laser cavity with Yb<sup>2+</sup> glass and (c) Superbroadband fluorescence of Yb<sup>2+</sup>-doped glass in the F-P cavity using 405 nm laser pump.



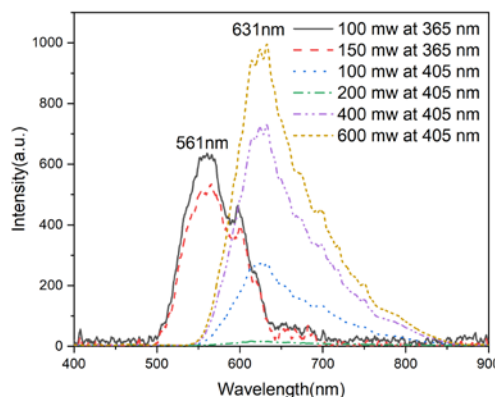
**Figure 6.** Harsh white light photograph of Yb<sup>2+</sup>-doped glass with excitation of 405 nm.

The structure of the  $\text{Yb}^{2+}$ -doped fiber fabricated by rod-in-tube technology is shown in Figure 7. The fiber core is  $\text{Yb}^{2+}$ -doped silica glass presented in Figure 1, and the fiber and fiber core diameters are 156.06 and 27  $\mu\text{m}$ , respectively. The refractive index profile of the  $\text{Yb}^{2+}$ -doped fiber is shown in Figure 7b. The black and red lines represent the horizontal and vertical refractive index profiles, respectively. The refractive index of the immersion liquid was 1.462. The  $\Delta n$  between the fiber core and fiber cladding was  $4.26 \times 10^{-4}$ , whereas it was  $2.737 \times 10^{-4}$  in the fiber core.



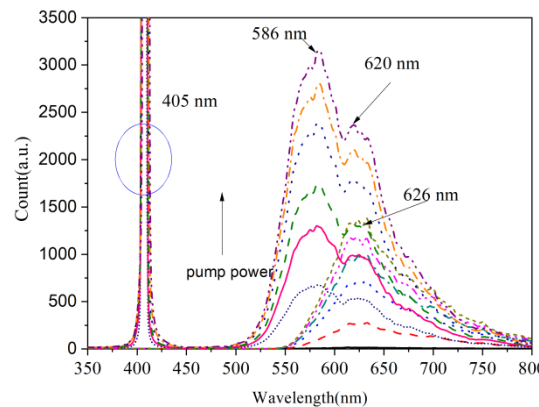
**Figure 7.** (a) Typical scanning electron microscopy image (scale bar of 30  $\mu\text{m}$ ) and (b) refractive index profile of the  $\text{Yb}^{2+}$ -doped fiber.

Figure 8 shows the emission spectra of  $\text{Yb}^{2+}$ -doped fiber with length of 30 cm and excitation of 365 nm and 405 nm as a function of pump power, 100 and 150 mW for 365nm laser, 100, 200, 400, and 600mW for 405 nm laser. Broad emission bands centred at 561 nm are observed with the excitation of 365 nm, which is attributed to the typical  $4\text{f}^{13}5\text{d}^1 - 4\text{f}^{14}$  transitions of  $\text{Yb}^{2+}$  ions [21]. The emission band covers wavelengths from 500 to 650 nm, the full width at half maximum (FWHM) of the emission band is up to 82 nm. This suggest that the  $\text{Yb}^{2+}$ -doped fiber can be used to produce tunable fiber lasers operating at visible region. When the excitation wavelength is 405 nm, broad emission bands centred at 631 nm are also observed. The emission band covers wavelengths from 550 to 850 nm, the FWHM of the emission band is up to 91 nm. These results suggest that  $\text{Yb}^{2+}$ -doped silica fiber can be used to produce tunable fiber lasers operating at visible region.



**Figure 8.** Emission spectra of  $\text{Yb}^{2+}$ -doped fiber with length of 30 cm as a function of pump power with excitation of 365 and 405 nm.

Emission spectra of  $\text{Yb}^{2+}$ -doped fiber with lengths of 30 and 60 cm as a function of pump power at the excitation of 405 nm are shown in Figure 9. As seen, the emission spectra for different lengths are different. When the length of the fiber is short, there are two emission peaks centred at 586 and 620 nm. The FWHM of the emission band is up to 108 nm, and the wide emission bands suggest that  $\text{Yb}^{2+}$ -doped fiber can be used to produce a tunable fiber laser operating in the visible region. When the fiber length is longer, the centred wavelength of the emission band shifts to 626 nm, which is in agreement with the results in reference [4]. As the fiber length increases, the emission wavelengths shift to longer wavelengths. In addition, with the increase in pump power, the emission band centred wavelength also shifts to longer wavelengths.



**Figure 9.** Emission spectra of  $\text{Yb}^{2+}$ -doped fiber lengths of 30 and 60 cm as a function of pump power at the excitation of 405 nm.

To study the laser performance of the  $\text{Yb}^{2+}$ -doped fiber, a free-space laser resonator cavity was constructed with an  $\text{Yb}^{2+}$ -doped fiber of 30 cm. The laser experiment setup is shown in Figure 10. The cavity was constructed with two dichroic mirrors with high reflectivity (>99% and 85%) at 561 nm. The pump source was a 405 nm laser diode with a laser spot diameter of 105  $\mu\text{m}$  and numerical aperture of 0.22. The pump light was collimated and focused into the inner cladding of the fiber by an 8X objective lens. Figure 11 shows the change in the emission spectra as a function of the angle between the fiber face and laser cavity mirror. As shown in Figure 11, with a reduction in the angle, the intensity of the emission spectra increases. Two emission peaks centred at 635 and 679 nm are observed. Moreover, as the angle increases, the emission peak centred at 679 nm disappears, and only the emission peak centred at 635 nm is observed, which suggests that a free-space laser resonator cavity is reformed. Figure 12 shows the intense emission peak centred at 637 nm as a function of pump power with an excitation of 405 nm. However, because the available pumping power was limited, a remarkable laser emission could not be observed. The results of the experiments suggest that the  $\text{Yb}^{2+}$ -doped fiber laser operating at visible wavelength is feasible. In future works, more optical experiments on the  $\text{Yb}^{2+}$ -doped fiber will be performed for the fiber laser.

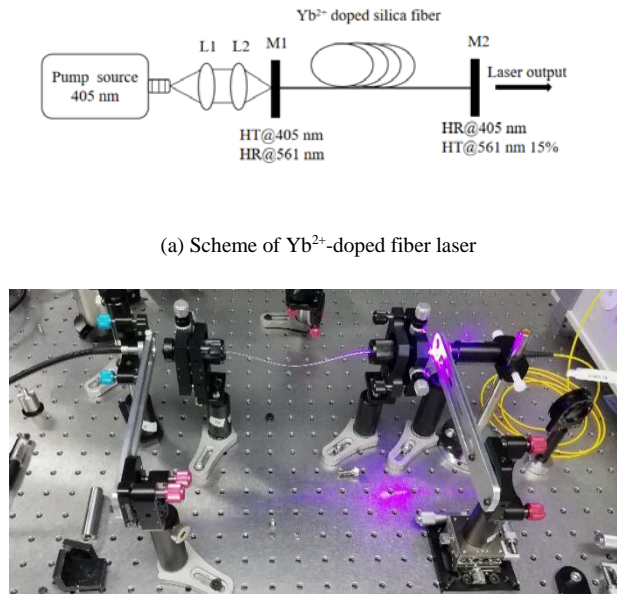


**Figure 10.** (a) Scheme and (b) setup of the  $\text{Yb}^{2+}$ -doped fiber laser.

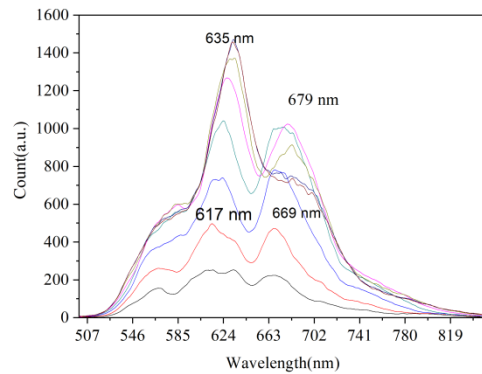


**Figure 11.** Emission spectra of the  $\text{Yb}^{2+}$ -doped silica fiber as a function of the angle between fiber face and laser cavity mirror at an excitation of 405 nm.

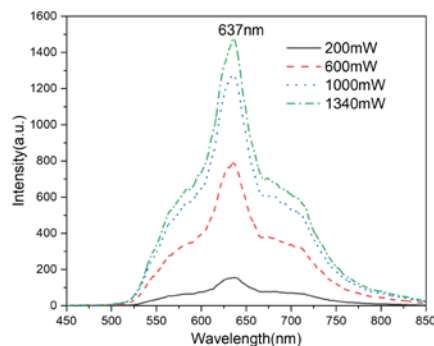


**Figure 12.** Emission spectra of the  $\text{Yb}^{2+}$ -doped silica fiber as a function of pump power at an excitation of 405 nm

## 5. Conclusions

A divalent Yb<sup>2+</sup>-doped silica fiber for a white light source was fabricated by the rod-in-tube method. The Yb<sup>2+</sup>-doped silica glass for the fiber core was prepared by high-temperature melting technology under vacuum conditions. The spectroscopic properties of Yb<sup>2+</sup>-doped glass and fiber were studied. An intense emission peak centred at 637 nm was observed in the divalent Yb<sup>2+</sup>-doped fiber. The results show that the divalent Yb<sup>2+</sup>-doped glass has a high quantum efficiency and superbroadband fluorescence in the visible region with an excitation wavelength of 405 nm. The laser experiment for Yb<sup>2+</sup>-doped silica fiber was performed; however, because the available pumping power was limited, a remarkable laser emission could not be observed. In future works, more optical experiments on the Yb<sup>2+</sup>-doped fiber will be performed in order to obtain the fiber laser. Based on the above results, these experiments suggest that Yb<sup>2+</sup>-doped silica and fiber have potential applications in visible fiber laser and amplification.

## 6. Acknowledgments

This work was supported by the National Natural Science Foundation of China (Grant No. 61935010). We would like to thank Editage (www.editage.cn) for English language editing.

## 7. Disclosures

The authors declare no conflicts of interest.

## References

1. S. Kück, "Laser-related spectroscopy of ion-doped crystals for tunable solid-state lasers", *Appl. Phys. B* 72(5), 515-562 (2001).
2. J. Kirchhof, S. Unger, S. Jetschke, V. Reichel, M. Leich, "The influence of Yb<sup>2+</sup> ions on optical properties and power stability of ytterbium-doped laser fibers", *Proc. Spie.* 7598(2), 75980B-75980B-75911 (2010).
3. S. Wang, F. Lou, C. Yu, Q. Zhou, M. Wang, S. Feng, D. Chen, L. Hu, W. Chen, M. Guzik, "Influence of Al<sup>3+</sup> and P<sup>5+</sup> ion contents on the valence state of Yb<sup>3+</sup> ions and the dispersion effect of Al<sup>3+</sup> and P<sup>5+</sup> ions on Yb<sup>3+</sup> ions in silica glass", *J. Mater. Chem. C* 2(22), 4406 (2014).
4. C. Xia, G. Zhou, H. Ying, X. Zhao, L. Hou, "Luminescence of Yb<sup>2+</sup>, Yb<sup>3+</sup> co-doped silica glass for white light source", *Opt. Mater.* 34(5), 769-771 (2012).
5. I. Nicoara, L. Lighezan, M. Enculescu, I. Enculescu, "Optical spectroscopy of Yb<sup>2+</sup> ions in YbF<sub>3</sub>-doped CaF<sub>2</sub> crystals", *J. Cryst. Growth* 310(7-9), 2026-2032 (2008).
6. C. Mackeen, F. Bridges, M.E. Kozina, A. Mehta, Z. Barandiaran, "Evidence That the Anomalous Emission from CaF<sub>2</sub> :Yb<sup>2+</sup> Is Not Described by the Impurity Trapped Exciton Model", *J. Phys. Chem. Lett.* 8(14), 3313 (2017).
7. E. Loh, "Strong-Field Assignment on 4f<sup>13</sup>5d Levels of Yb<sup>2+</sup> in SrCl<sub>2</sub>", *Phys. Rev. B* 7(5), 1846-1850 (1973).
8. S. Kück, M. Henke, K. Rademaker, "Crystal growth and spectroscopic investigation of Yb<sup>2+</sup>-doped fluoride crystals", *Laser Phys.* 11(1), 116-119 (2001).
9. M. Henke, J. Persson, S. Kück, "Preparation and spectroscopy of Yb<sup>2+</sup>-doped Y<sub>3</sub>Al<sub>5</sub>O<sub>12</sub>, YAlO<sub>3</sub>, and LiBaF<sub>3</sub>", *J. Lumin.* 87(5), 1049-1051 (2000).
10. M. Hendriks, E. van der Kolk, "4f→5d and anomalous emission in Yb<sup>2+</sup> doped NaI, SrI<sub>2</sub> and LaI<sub>3</sub> powders prepared by rapid melting and quenching in vacuum", *J. Lumin.* 207, 231-235 (2019).
11. Y. Huang, P. Wei, S. Zhang, H.J. Seo, "Luminescence Properties of Yb<sup>2+</sup> Doped NaBaPO<sub>4</sub> Phosphate Crystals", *J. Electrochem. Soc.* 158(5), H465 (2011).
12. A. Assadi, A. Herrmann, K. Damak, C. Rüssel, R. Maalej, "Spectroscopic properties of Yb<sup>2+</sup> in aluminosilicate glass", *Int. J. Appl. Glass Sci.* 8(3), 1-7 (2017).
13. C. Xia, G. Zhou, Y. Han, X. Zhao, C. Wang, L. Hou, "Investigation on preparation and spectroscopic properties of Yb<sup>2+</sup>-doped silica-based glass prepared by the oxyhydrogen flame fusing process", *Opt. Mater.* 35(12), 2561-2564 (2013).
14. S. Liu, S. Zheng, C. Tang, X. Li, W. Xu, Q. Sheng, D. Chen, "Photoluminescence and radioluminescence properties of Yb<sup>2+</sup>-doped silica glass", *Mater. Lett.* 144, 43-45 (2015).
15. M. A. Mittsev, M.V. Kuz'Min, M.V. Loginov, "Mechanism of the Yb<sup>2+</sup>→Yb<sup>3+</sup> valence transition in ytterbium nanofilms upon chemisorption of CO and O<sub>2</sub> molecules on their surface", *Phys. Solid State* 58(10), 2130-2134 (2016).

16. P. Quinet, P. Palmeri, E. Biémont, Z. Li, Z. Zhang, S. Svanberg, "Radiative lifetime measurements and transition probability calculations in lanthanide ions", *J. Alloys. Compd.* 344(1-2), 0-259 (2002).
17. Z. Li, Z. Zhang, V. Likhnygin, S. Svanberg, T. Bastin, E. Biémont, H. Garnir, P. Palmeri, P. Quinet, "Radiative lifetime measurements in Tm III with time-resolved laser spectroscopy and comparisons with HFR calculations", *J. Phys. B. Atom. Molec. Opt. Phys.* 34(8), 1349 (2001)
18. Z. Li, Z. Chen, Y. Yang, Q. Xue, H. Yip, Y. Cao, "Modulation of recombination zone position for quasi-two-dimensional blue perovskite light-emitting diodes with efficiency exceeding 5%", *Nat. Commun.* 10(1), 1027 (2019).
19. Y. Cheng, H. Su-Juan, M. Zhuang, C. Zheng, Z. Jun-Zhang, W. Ting-Yun, "3D refractive index measurements of special optical fibers", *Opt. Fiber Techn.* 31(sep.), 65-73 (2016).
20. Z. Zhang, O. Ten Kate, A. Delsing, Z. Man, R. Xie, Y. Shen, M. Stevens, P. Notten, P. Dorenbos, J. Zhao, "Preparation, electronic structure and photoluminescence properties of RE (RE = Ce, Yb)-activated SrAlSi<sub>4</sub>N<sub>7</sub> phosphors", *J. Mat. Chem. C* 1(47), 7856 (2013).
21. X. Wang, Ch. Ma, X. Xu, Zh. Zhao, J. Xu, "Spectroscopic and Laser Properties of Yb:Lu<sub>3</sub>Al<sub>5</sub>O<sub>12</sub> Crystal under Different Annealing Atmospheres", *Chin. J. Lasers* 37(4), 1099-1103 (2010).